Journal of Catalysis **198,** 328–337 (2001)
doi:10.1006/jcat.2000.3152, available online at http://www.idealibrary.com on IDEAL®

Isomerization of *n*-Hexane over Sulfated Zirconia: Influence of Hydrogen and Platinum

J. C. Duchet,*,[1] D. Guillaume,* A. Monnier,* C. Dujardin,* J. P. Gilson,* J. van Gestel,* G. Szabo,† and P. Nascimento†

* *Laboratoire Catalyse et Spectrochimie, UMR CNRS 6506, ISMRA-Université, 6, Bvd. Maréchal Juin, 14050 Caen Cedex, France; and* †*CERT, TotalFinaElf, 76700 Harfleur, France*

Received September 15, 2000; accepted November 30, 2000; published online February 15, 2001

Isomerization of *n*-hexane (1–5 bar) is studied over sulfated zirconia at 423 K and 50 bar, under 5–45 bar hydrogen. The sulfated zirconia is crystallized at 923 K, then loaded with 0.025–0.8 wt% platinum. The isomerization rate first increases with hydrogen pressure, reaches a maximum, and finally decreases slowly. At a given platinum content, the position of the maximum increases with hexane pressure. The shape of the activity curves versus hydrogen partial pressure depends strongly on the platinum content. All the activity data are kinetically modeled by an acid mechanism in which the Lewis acid–base sites create carbenium ions. Activated hydrogen on platinum spills over to form the hydride species responsible for the desorption of the isocarbenium ions. The three parameters of the rate equation reflect the number of sites, the acid strength, and the efficiency of platinum. In the series of catalysts examined, the acidity is constant while the platinum efficiency increases with loading and reaches an upper limit at 0.15% platinum loading.

Key Words: **sulfated zirconia; isomerization; Lewis acidity; platinum; kinetics; mechanism.**

INTRODUCTION

The existing and forthcoming regulations on gasoline have highlighted the need for "clean" high-octane molecules in the gasoline pool. Isoparaffins produced by alkylation of butene by isobutane and isomerization of the C_5–C_7 cut have the right combination of RON/MON properties and compliance with environmental regulations. Solid acid catalysts are required for their production and a renewed interest in their use is noticeable in the last few years. Among them, sulfated zirconia is very attractive since it offers a nice alternative for the corrosive halogen-containing solid acids in the skeletal isomerization of light linear alkanes at low temperature. Recently, UOP has marketed sulfated zirconia catalysts for this purpose (1). Much work has been devoted to sulfated zirconia and compiled in several reviews (2–7). In the present work, we focus on the influence of platinum and hydrogen on the reaction mechanism. Addition of platinum and hydrogen is required to prevent the rapid deactivation of the catalyst. The role of platinum in the presence of hydrogen is still a controversial issue. Some authors report that platinum brings the metallic function in a classical bifunctional mechanism (8). Ebitani *et al.* (9–11) observe a promoting effect of hydrogen on the isomerization. They suggest that strong protonic acidity is generated via dissociation and spillover of hydrogen species. Iglesia *et al.* and Comelli *et al.* (12–14) also observe a promoting effect of Pt and H_2 and attribute it to the conversion of hydrogen atoms into hydrides, accelerating the desorption of the carbenium intermediates. In these studies, the influence of hydrogen is always limited to low hydrogen pressures.

We recently reported that much valuable information on the role of platinum and hydrogen is obtained from the catalytic transformation of *n*-hexane under a wide range of hexane and hydrogen partial pressures (15, 16). Platinum calcination and reduction temperatures have a dramatic influence on the catalytic activity. The kinetic modeling yields a very simple rate equation describing these effects. This paper develops more exhaustively the reaction mechanism and the kinetic treatment and extends the studies to catalysts containing various amounts of Pt.

EXPERIMENTAL

Catalyst Preparation

Zirconium hydroxide is precipitated from an aqueous solution of zirconium oxychloride by ammonium hydroxide. The dry material is sulfated by pouring in a 0.5 M H_2SO_4 solution, filtering, and drying. The powder is then shaped by extrusion (5×1.6 mm) by mixing it with 20% xerogel alumina, followed by calcination at 923 K. The sulfur content amounts to 2.0 wt%, as analyzed at the CNRS (Vernaison). Platinum (0.025–0.8 wt%) is loaded by impregnation with an H_2PtCl_6 solution. The final catalysts are calcined at 753 K.

[1] To whom correspondence should be addressed. Fax number: 33 2 31 45 28 22. E-mail: duchet@ismra.fr.

0021-9517/01 $35.00

Three other samples are prepared without alumina binder for FTIR characterization of adsorbed CO. Zirconium hydroxide is prepared as described above. A sample of pure ZrO_2 is obtained by calcining the hydroxide at 773 K. The sample SO_4–ZrO_2 is prepared by sulfatation of the dry hydroxide with H_2SO_4, followed by calcination at 923 K. The third sample Pt–SO_4–ZrO_2 is prepared by impregnating the calcined SO_4–ZrO_2 sample with 0.45% Pt and then calcining it at 753 K.

Activity Measurement

The extrudates (0.5 g) are activated in the flow reactor at 673 K for 2 h in a dry air stream (50 ml/min) and contacted with flowing hydrogen (70 ml/min) at 423 K for 1 h. Dry *n*-hexane (1, 3, and 5 bar) is vaporized in the dry hydrogen–helium mixture at 50 bar total pressure and 423 K. The hydrogen partial pressure is varied from 5 to 45 bar. The reaction products are analyzed online with a Varian 3400 GC equipped with a CPSIL-5B capillary column and an FID detector. Analyses are performed automatically every hour. Sampling starts at steady state, after 0.6 h. The catalyst is stable over at least 1 week. Eventually, complete regeneration is obtained by calcination *in situ* under flowing dry air at 673 K. Conversions are kept in the range 10–35%. The reaction follows an order close to 1, which is used to calculate initial rates.

Infrared Characterization

Infrared spectra are recorded with a Nicolet Magma 550 spectrometer equipped with an MCT detector. The alumina-free or alumina-bound catalysts are pressed into self-supported wafers, activated *in situ* under 100 Torr of O_2 at 773 K and evacuated at 773 K. The catalysts are contacted at 100 K (acidity measurements) or at room temperature (Pt site characterization) with 1 Torr of CO at equilibrium. Spectra are then recorded after evacuation either at 100 K or at room temperature.

XRD Characterization

Powder X-ray diffraction spectra are recorded on a Philips PW1750 spectrometer using Cu$K\alpha$ radiation. Each step of 0.02° from 20 to 70° (2θ) is measured for 5 s.

RESULTS AND DISCUSSION

The kinetic and mechanistic study of the isomerization of *n*-hexane reported here is based on activity data collected on sulfated zirconia catalysts shaped as extrudates with an alumina binder. These conditions of measurement are closely representative of industrial reactors, which cannot operate with powdered catalysts. Since the mechanical properties of pure zirconia extrudates are very poor, mixing with 20% binder is necessary. Such a shaping could modify the properties of the zirconia; it is argued below that our procedure does not induce such changes.

From the literature, incorporation of alumina to zirconia strongly depends on the preparative conditions. Coprecipitation of the two hydroxides (17) yields a mixed oxide system, in which aluminium ions retard the dehydration upon drying and hamper the growth of the small tetragonal crystallites of zirconia upon calcination. The system becomes amorphous, loses its Lewis acidity and its catalytic properties for butane isomerization. Stabilization of zirconia in the amorphous state can also be obtained by simple impregnation of the dry zirconium hydroxide with aluminium nitrate followed by calcination (18).

Zalewski *et al.* (19) reported that a prolonged mixing of the two hydroxides in the presence of large amounts of water and subsequent calcination at 873 K incorporates alumina. Again, sintering of the active tetragonal crystallites of zirconia is suppressed, and the lifetime of the catalyst for alkylation is increased.

In our case, the two dried hydroxides are mixed with a minimum of water to form a paste, which is extruded. XRD spectra evidence crystalline zirconia after calcination at 923 K for both plain sulfated zirconia and sulfated zirconia bound with alumina (Fig. 1). Apart from a small fraction of monoclinic zirconia, we identify the cubic phase from the diffraction line at $2\theta = 63°$ (20). Moreover, the weight-averaged intensity of the diffraction lines, corrected for the zirconia content, is unaffected by the presence of the binder. The crystallite size, evaluated from the Scherrer formula, is constant at around 100 Å for both types of samples. This strongly suggests a biphasic system and a physical effect of the binder.

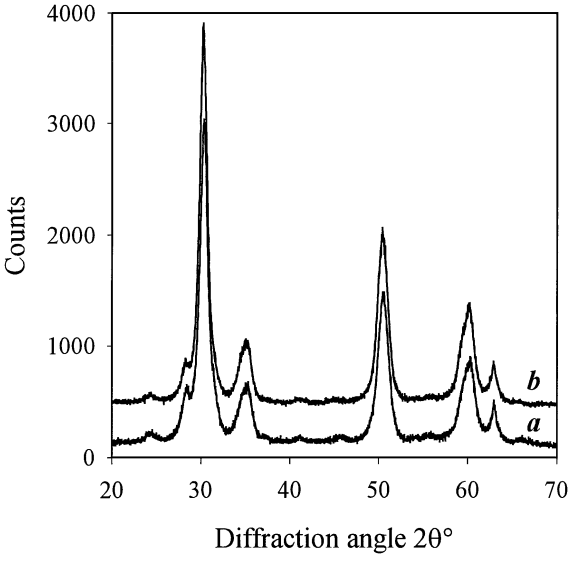

FIG. 1. XRD spectra for SO_4–ZrO_2 (a) and SO_4–ZrO_2 extruded with alumina (b).

Although we cannot exclude some surface incorporation of alumina, our preparation conditions should limit it to a very low fraction. Moreover, all the samples of the series studied here differ only by their platinum content and are prepared by impregnation of the same sulfated zirconia–alumina extrudates. Hence, the influence of alumina, if so, is constant within the series and allows study of the influence of hydrogen and platinum.

CATALYST CONTAINING 0.3% PLATINUM

Product Distribution

Figure 2 shows the product distribution observed for the catalyst containing 0.3% Pt. Cracking is negligible. The figure illustrates the isomer distribution measured at various contact times and hydrogen pressures. Methyl-2-pentane (2MP), methyl-3-pentane (3MP), and dimethyl-2,3-butane (23DMB) are the primary products and are present at their thermodynamic ratio. Dimethyl-2,2-butane (22DMB) is clearly a secondary product. We would expect 23DMB to also be a secondary product. However, it is rapidly equilibrated with 2MP and 3MP, indicating that the first steps in isomerization are quite fast. The selectivity is influenced neither by the platinum content nor by the hydrogen partial pressure.

Influence of Hydrogen Pressure

The influence of hydrogen pressure on isomerization rate is shown in Fig. 3 for the catalyst containing 0.3% platinum.

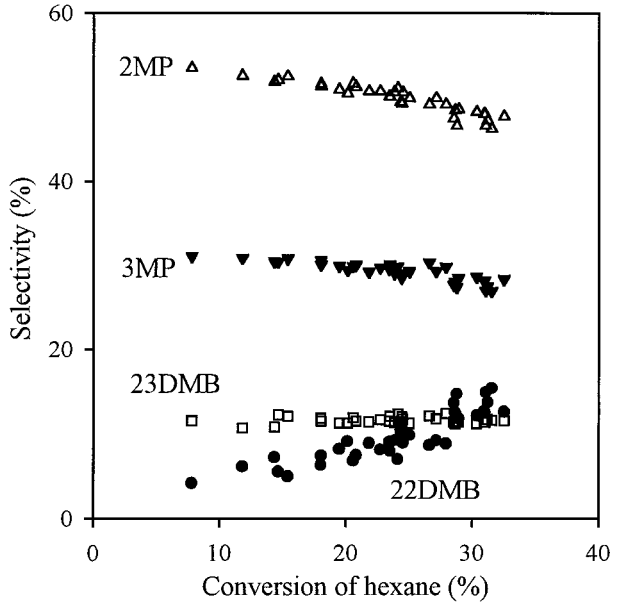

FIG. 2. Product distribution at 423 K for Pt(0.3%)–SO_4–ZrO_2 at various contact times and hydrogen pressures (2–45 bar): 2-methylpentane (△), 3-methylpentane (▼), 2,3-dimethylbutane (□), 2,2-dimethylbutane (●).

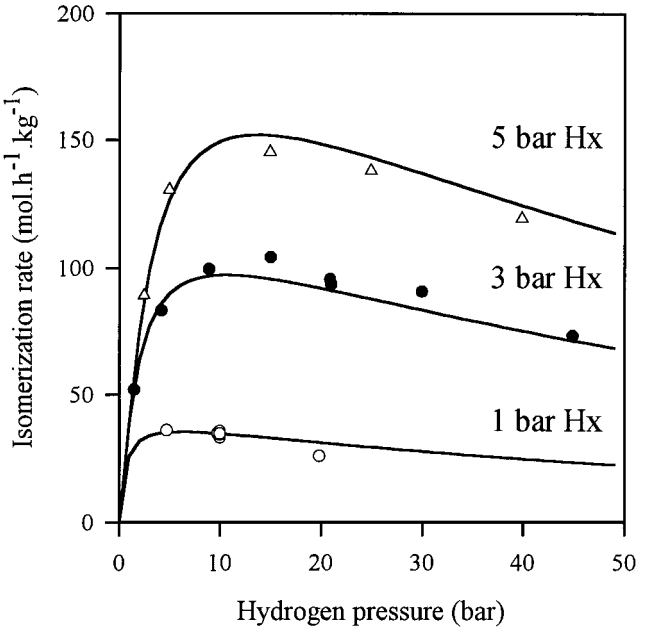

FIG. 3. Influence of hexane and hydrogen partial pressures on the isomerization rate for Pt(0.3%)– SO_4–ZrO_2. Hexane pressures: 1 bar (o), 3 bar (●), 5 bar (△).

The reaction is not observed without hydrogen. At a given hexane pressure, the rate strongly increases up to a maximum and then slowly decreases. The position of the maximum shifts from 3 to 15 bar hydrogen with increasing hexane pressure in the range 1–5 bar. The reaction order with respect to *n*-hexane is slightly lower than 1 at low hydrogen pressure and reaches 1 beyond the maximum.

Infrared Spectra of Adsorbed Carbon Monoxide

Infrared spectroscopy of adsorbed carbon monoxide is first used to detect Lewis acid sites of the sulfated zirconia. Spectra a and b in Fig. 4 compare in the region 2200 cm^{-1} two sulfated samples, with and without alumina binder, activated at 773 K. CO was adsorbed at equilibrium at 100 K and evacuated. Under these conditions, pure alumina does not retain carbon monoxide, and no signal for adsorption on the alumina component of the sample was detected. Clearly, the two spectra show the same band at 2204 cm^{-1} assigned to CO adsorption on coordinatively unsaturated zirconium. The difference in intensity of the signals reflects the proportion of zirconia in the two samples. Therefore, the alumina binder does not influence the Lewis acidity of the sulfated zirconia, despite its high proportion (20%). According to Ref. (17), CO adsorption on sulfated zirconia is unaffected by incorporation of alumina up to 3 mol% in zirconia–alumina systems prepared by coprecipitation. Our samples are prepared by extrusion under conditions far less favorable than those of the coprecipitation method for incorporating alumina. Hence, they should incorporate much less alumina, if any. The spectrum of pure zirconia shown

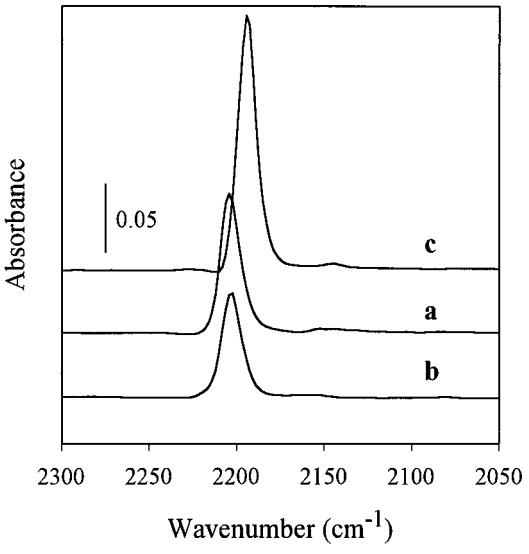

FIG. 4. FTIR spectra of adsorbed CO at 100 K and evacuated at 100 K. (a) SO_4–ZrO_2, (b) SO_4–ZrO_2, (c) ZrO_2 extruded with alumina.

in Fig. 4c presents a CO band at 2194 cm^{-1}. Compared to the sulfated oxide, sulfating induces a shift to 2204 cm^{-1} in agreement with the literature (21–23). It points to an enhancement of the Lewis acid strength. The bands totally disappear upon rising temperature at ambient and evacuation.

The spectrum of CO adsorbed at 100 K on the Pt(0.45%)–SO_4–ZrO_2 sample presented on Fig. 5a shows bands at 2204, 2154, and 2097 cm^{-1}. Evacuation at room temperature (Fig. 5b) does not affect the position and intensity of the bands at 2154 and 2094 cm^{-1}, while the one at 2204 cm^{-1} disappears and a new signal of low intensity appears at 2194 cm^{-1}. Since the Pt-free samples show no bands of adsorbed CO in this region after evacuation at room temperature, the remaining bands on the platinum-containing sample should be attributed exclusively to several Pt species. So, we can evidence the band of adsorbed CO at low temperature characteristic of the Lewis sites by subtracting the spectrum of the Pt-containing sample at room temperature from the spectrum evacuated at 100 K. This yields the proper adsorption band at 2204 cm^{-1} of the Lewis acid sites on the Pt-loaded sulfated zirconia (Fig. 5c). So, the presence of 0.45% platinum does not affect the acid strength of the sulfated zirconia. After reduction at 423 K, the platinum sample shows only a band at 2080 cm^{-1} characteristic of metallic Pt (spectra not shown). Similarly, platinum does not influence the sulfate bands (spectra not shown). Under these activation conditions, no bands characteristic of hydrogenosulfates are detected.

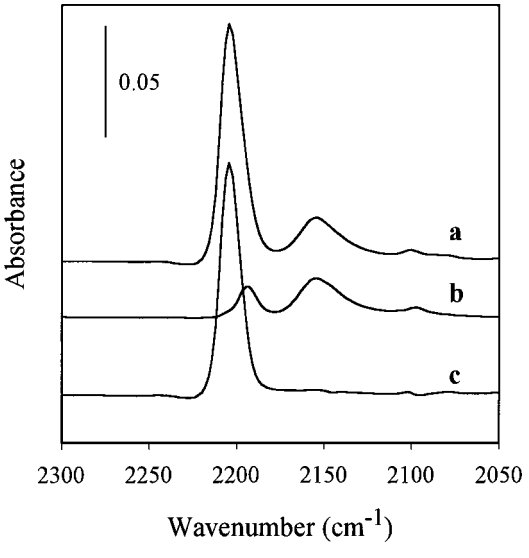

FIG. 5. FTIR spectra of adsorbed CO at 100 K on the Pt(0.45%)–SO_4–ZrO_2 sample. (a) Evacuated at 100 K, (b) evacuated at 298 K, (c) subtraction result a − b.

Reaction Mechanism

Several types of mechanisms could account for the main feature of the experimental data: a change in hydrogen order, from positive to negative. This maximum in activity with hydrogen pressure over metal–acid catalysts has been scarcely reported in the literature so far. The two widely reported mechanisms, namely, the bifunctional mechanism and the acidic mechanism on Brønsted sites, are first discussed and then a new mechanism based on the spectroscopic evidences provided above is presented.

Bifunctional Mechanism

Bifunctional reforming catalysts give a first example of the influence of hydrogen on the dehydrocyclization of *n*-heptane at high temperature (24). Their low activity at low hydrogen partial pressure is classically interpreted by coke formation. Increasing hydrogen partial pressure prevents such a side reaction. Finally, high hydrogen partial pressure slightly inhibits the reaction, the dehydrogenation step of the hydrocarbon into an olefin being unfavorable. More recently, a maximum in isomerization rate of light alkanes on platinum–zeolite catalysts operating at 523 K (25) has also been interpreted by a classical metal–acid bifunctional mechanism. Besides the well-known negative effect of hydrogen on the olefin formation, the authors introduce a further dehydrogenation step into a diolefin to account for a positive effect at low hydrogen pressure. The authors propose the rate expression

$$r = \frac{k \cdot (\mathrm{RH}) \cdot (\mathrm{H})}{(\mathrm{H})^2 + (\mathrm{RH}) \cdot (a \cdot (\mathrm{H}) + b)}, \qquad [1]$$

where (RH) and (H) stand for the hydrocarbon and hydrogen partial pressures, respectively. They have checked qualitatively the reaction orders predicted by the rate

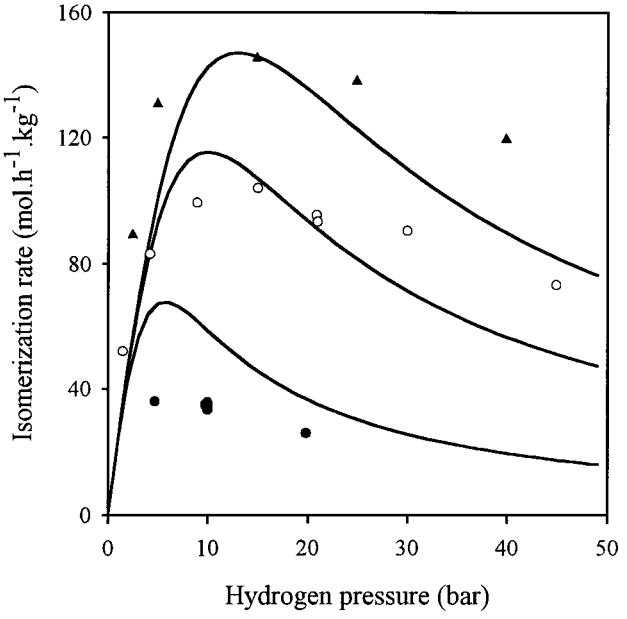

FIG. 6. Application of the rate equation (Eq. 1) for the bifunctional mechanism (25) to isomerization data obtained with the catalyst Pt(0.3%)–SO_4–ZrO_2. Hexane pressures: 1 bar (●); 3 bar (o); 5 bar (▲).

equation, yielding a maximum in the curves. We tried to apply this equation to our data by optimizing the corresponding kinetic parameters. We found that the model gives a good fit only for the data obtained at one given pressure of hexane, but, as shown in Fig. 6, it completely fails to fit the whole range of hexane pressures. Clearly, it does not account for the hexane reaction order on sulfated zirconia at 423 K. We attempted to adjust the olefin–diolefin ratios in several reaction schemes but none of the resulting rate equations models our data. Therefore, a classical bifunctional metal–acid mechanism is improbable at 423 K over platinum-sulfated zirconia catalysts, even if the samples show platinum in the metallic state after contacting the catalyst with hydrogen. A similar conclusion, based on the very low concentration of the olefin intermediate, is reported in the literature (12, 26).

The role of platinum in Pt–SO_4–ZrO_2 catalysts should therefore be focused on the activation of hydrogen. This important aspect of the working catalyst has been considered by some authors (10, 12–14, 27) to explain the positive hydrogen order. Two pictures emerge from these studies. According to Ebitani *et al.* (11), hydrogen is a source of Brønsted acidity, as evidenced by infrared spectroscopy. Molecular hydrogen is homolytically dissociated on platinum, and the atoms migrate by spillover to the sulfated zirconia sites where they convert either into H^+ and H^- or $2H^+$ and $2\ e^-$. Protons and hydrides affect the balance between the Lewis and Brønsted sites. Brønsted acidity is enhanced as is the activity.

The approach of Iglesia *et al.* (12) is different. Studying *n*-heptane isomerization at 473 K on Pt–SO_x–ZrO_2, they draw a parallel between the positive effect brought by hydrogen and adamantane. Since the latter is known as a hydrogen donor, they conclude that in both cases hydrides play a direct role in the reaction by desorbing the isomerized carbenium ions. The hydride species shorten the residence time of the carbenium species on the sulfated zirconia surface and therefore minimize polymerization and cracking (10, 13, 14). Several steps convert molecular hydrogen into the active hydride species: dissociative H_2 adsorption on the Pt surface, conversion into hydrides and Pt^+, and finally transfer to the adsorbed carbenium ion on the acidic site.

Both interpretations account for a positive effect of hydrogen and are satisfactory as long as the hydrogen pressure is not too high. The difficulty arises with the maximum in hydrogen pressure. For a complete kinetic modeling, we have to establish the whole sequence of elementary steps, which is the subject of the following paragraph.

Acidic Mechanism on Brønsted Sites

The sequence starts with the initiation step. The formation of the initial carbenium ion is commonly described via a carbonium intermediate on Brønsted acid sites (4).

$$RH + H^+ \rightarrow RH_2^+ \rightarrow R^+ + H_2$$

This requires a strong acidity. Indeed, many reviews in the literature ascribe a superacidity to these solids (28, 29). Although it is not our purpose here to describe the exact interaction of the sulfate species with zirconia, IR studies in our laboratory identified several hydrogenosulfate species (30). An acidity as low as $H_0 = -13$ on the Hammett scale is measured by protonation of chloroacetonitrile. However, activation at higher temperatures transforms this Brønsted acidity into Lewis acidity by elimination of water.

The next step isomerizes the carbenium. This step is equilibrated since the primary hexane isomers are in thermodynamic equilibrium.

$$R^+ \leftrightarrow iR^+$$

Finally, the sequence ends by desorption of the isocarbenium. Classically, this can be achieved by a hydride transfer from the hydrocarbon, while regenerating the initial carbenium.

$$iR^+ + RH \rightarrow iRH + R^+$$

Unfortunately, such an isomerization sequence does not give a rate expression fitting our activity data. Another possibility would be desorption by hydride species, which can be formed by hydrogen dissociation on platinum. According to Iglesia *et al.* (12), hydride species are more active than hydrocarbon in desorbing the isocarbenium. However, including a desorption step by hydrides does not improve the rate expression to fit our data. Moreover, we tested a large number of rate equations based on Brønsted acidity at the initiation step. None of them gave a satisfactorily fit

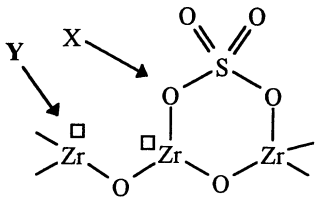

SCHEME 1. Plausible Lewis active sites (adapted from Ref. 32).

for the whole set of data. We conclude that the Brønsted acidity is not the key point to describe the working catalyst.

Acidic Mechanism on Lewis Sites

Alternatively, some authors emphasize the participation of Lewis sites in the reaction mechanism for alkane isomerization (31, 32). Indeed, the conversion of Brønsted species into Lewis sites readily occurs upon heating, as shown by FTIR (28–30). The infrared characterization of our sample by CO adsorption also indicates Lewis sites. Under our reaction conditions, activation of the catalyst is carried out *in situ* at 673 K in flowing dry air. Despite an activation temperature lower than that for IR measurements, Lewis sites most probably are present on the working catalysts. Several structures with Lewis sites are proposed in the sulfated zirconia literature. A plausible configuration adapted from the group of Morterra (32) (Scheme 1) is illustrative for the acid–base pair. It represents the Lewis acid (Zr) and base (O) sites (here denoted Y and X, respectively) required to write a reaction sequence.

We consider the Lewis acid–base pair as the active site. Isomerization starts by hydride abstraction from the hydrocarbon on coordinatively unsaturated Zr atoms (Y sites). This creates the carbenium ion which is stabilized on the Lewis basic sites (X sites) as already described (32, 33). Isomerization then rapidly occurs in a quasi equilibrium as before and, finally, the isocarbenium ion is desorbed by the hydride species created in the initiation step. This is a closed sequence depicted in Scheme 2. The three steps proceed at the same rate.

Such a sequence is consistent with the poisoning effect of water, which adsorbs on the Lewis sites. In principle the sequence operates in the absence of hydrogen. However, we could not measure any activity at steady state. We speculate that the desorption step is then too slow, leading to an accumulation of isocarbenium species on the surface and a fast deactivation.

$$\begin{aligned} X + Y + RH &\longrightarrow XR^+ + YH^- && k_i \\ XR^+ &\rightleftharpoons XiR^+ && K \\ XiR^+ + YH^- &\longrightarrow X + Y + iRH && k_t \end{aligned}$$

SCHEME 2. Isomerization sequence.

$$XY + H_2 \overset{Pt}{\longleftrightarrow} XH^+YH^- \qquad \alpha$$

SCHEME 3. Hydrogen activation.

The influence of hydrogen on the isomerization rate may be rationalized by a second sequence involving platinum (Scheme 3). Activation of hydrogen on platinum and migration to the active sites are necessarily equilibrated because there is no hydrogen consumption in the isomerization reaction. We find that the most satisfying rate equation is obtained by gathering in a single reaction the various steps of the platinum–hydrogen system: activation, migration, and conversion into hydride and proton species toward the acid–base sites of the sulfated zirconia. Formally, this corresponds to migration of hydrogen as a pair of atoms to reach the acid–base Lewis pair. Indeed, any attempt in which hydrogen atoms migrate separately on the sites leads to a rate expression containing a half order for the hydrogen term. This kind of expression does not fit the data.

Qualitatively, the Pt–hydrogen couple increases the concentration of hydride species. Then, it accelerates the desorption of isocarbenium ions. Coke formation is suppressed and isomerization can be observed. Moreover, it accounts for the positive order at low hydrogen pressure. The decrease in activity at higher hydrogen pressure is simply due to a competition between protons and carbenium species on the Lewis base sites, X.

The kinetic treatment by the stationary state of the combined sequences is detailed in the Appendix. In the termination step, we separate the contribution of the hydride species originating from hydrogen and from hydrocarbon in two desorption steps with rate constants k_{t1} and k_{t2}.

$$XiR^+ + YH^-_{Pt} \overset{k_{t1}}{\rightarrow} X + Y + iRH$$

$$XiR^+ + YH^-_{isom} \overset{k_{t2}}{\rightarrow} X + Y + iRH$$

Optimization of the kinetic parameters leads to a very low value of the ratio k_{t2}/k_{t1}. This yields the final rate expression

$$r = \frac{k \cdot (RH)}{\left\{1 + \alpha \cdot (H) + \frac{\beta}{\alpha} \cdot \frac{(RH)}{(H)}\right\}^2}, \qquad [2]$$

where $k = L k_i$ (L, number of adsorption sites), $\beta = (k_i/k_t)(1 + 1/K)$, (H) = pressure of hydrogen, and (RH) = pressure of hexane.

This equation predicts a maximum in rate for a hydrogen pressure proportional to $1/\alpha$. The curves in Fig. 3 are drawn after optimization of the kinetic parameters by nonlinear regression. All the data measured on the standard catalyst containing 0.3% Pt are fitted simultaneously. The fit is very satisfactory in the whole range of hexane pressures. The proposed mechanism is therefore plausible.

Chemically, the low value of the ratio k_{t2}/k_{t1} means that the desorption step by hydride species issued from the hydrocarbon is very slow and can be neglected. The stability of these species on the Zr Lewis acid site may be too high to ensure the termination step in the isomerization sequence. Only hydrides from hydrogen are active. This is consistent with the lack of activity in the absence of hydrogen. The sequence runs in the presence of hydrogen because the YH^- sites are liberated, presumably by reaction with protons, which are the counterions of the hydrides formed in the platinum–hydrogen system.

Besides the rate constant k, the two parameters α and β are well separated in the rate equation and should reflect any modification of the platinum–hydrogen efficiency (α) or of the Lewis acid–base pair (β). The validity of this equation has been checked on a series of samples with different platinum loading on the same sulfated zirconia.

INFLUENCE OF PLATINUM LOADING ON ISOMERIZATION

Platinum loading strongly changes the fingerprint of the catalyst activity. Figure 7 shows the isomerization rate at three hexane pressures for the catalyst containing only 0.025% Pt. Compared to the sample loaded with 0.3% Pt (Fig. 3), the increase in the rate with hydrogen pressure is much slower, and the maximum shifts to very high hydrogen pressure. But at a given hexane pressure, the maximum rate is not affected by the platinum content. The comparison of catalysts containing various platinum contents is shown in Fig. 8 for isomerization run at 3 bar hexane partial pressure. The change in curvature is gradual between 0.025 and 0.15% Pt with a maximum rate shifting downward to about 8 bar hydrogen. Again, the rate at maximum was not affected. Higher platinum loading does not change the pattern significantly. Only, a slight decrease in the maximum rate is observed. Then, the effect of platinum on isomerization readily reaches a limit for 0.15% Pt.

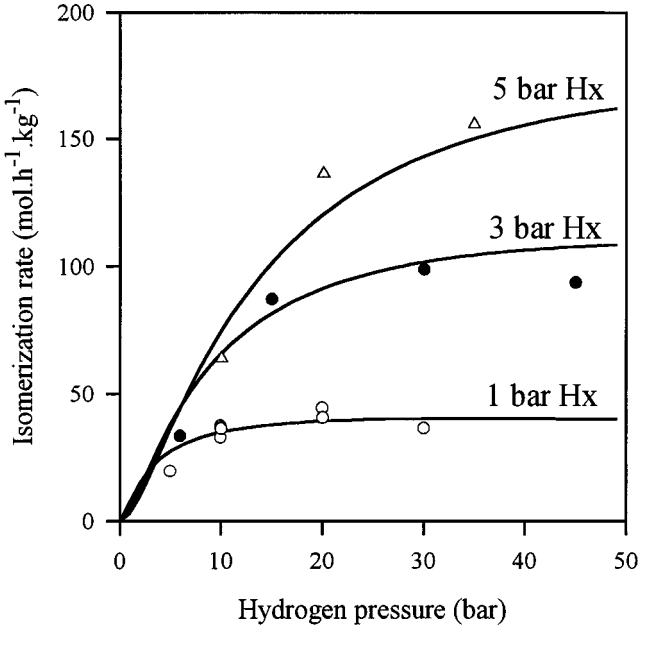

FIG. 7. Isomerization activity for the catalyst Pt(0.025%)–SO_4–ZrO_2 at three hexane pressures: 1 bar (o), 3 bar (●), 5 bar (△).

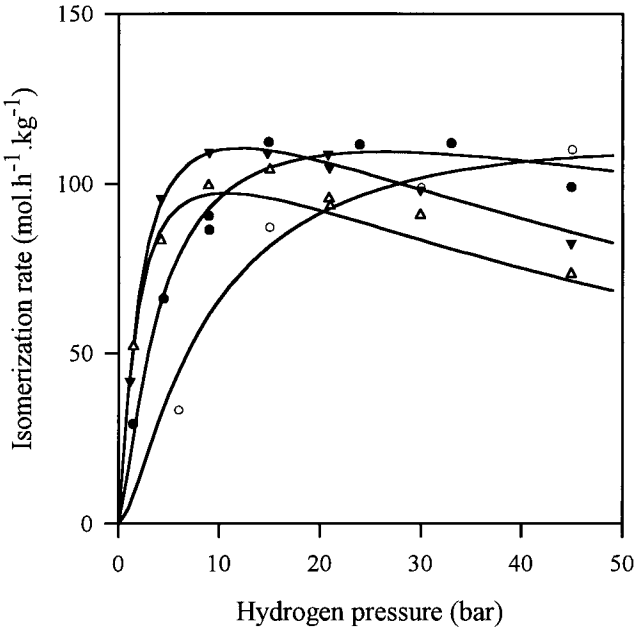

FIG. 8. Isomerization activity at 3 bar hexane over catalysts containing 0.025% (o), 0.10% (●), 0.15% (▼), and 0.50% Pt (△).

All the curves are fitted with the same rate equation developed in the preceding section. The effect of platinum is then quantified by the kinetic parameters. Optimized values are gathered in Table 1, and the evolution of the parameters with platinum loading is plotted in Fig. 9. It is first noticed that parameter β remains almost constant. This means that the strength of the Lewis sites of the sulfated zirconia is not altered by the presence of platinum. This is in line with the

TABLE 1

Kinetic Parameters of Eq. [2] for the Isomerization of *n*-Hexane on Sulfated Zirconia at 423 K

%Pt	k(mol h^{-1} kg^{-1})	$\alpha \times 10^3$ (bar^{-1})	$\beta \times 10^3$ (bar^{-1})
0.025	50	1.2	1.9
0.05	46	3.2	2.1
0.10	54	4.5	2.1
0.15	46	6.8	2.0
0.30	43	7.4	1.9
0.50	47	7.4	2.0
0.80	39	7.0	2.1

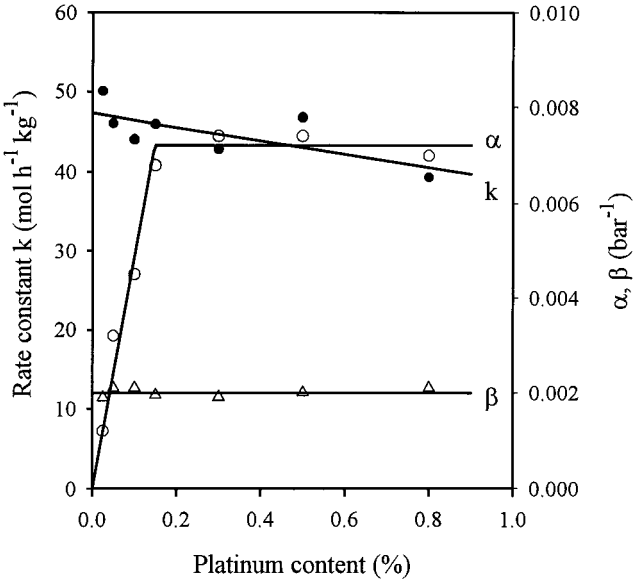

FIG. 9. Evolution of the kinetic parameters (Eq. 2) with platinum content: k (●), α(o), and β(Δ).

infrared characterization of the Lewis acid sites by CO adsorption shown in Fig. 5. Only, the number of the acid–base pairs slightly decreases as attested by the values of the rate constant k. The evolution of the parameter α in the series is remarkable. For low platinum loading, α increases rapidly up to 0.15% Pt, and stays constant beyond this value. According to the kinetic expression, α reflects the platinum efficiency. The variation of α should correspond to a linear increase in hydride concentration at low Pt loading, followed by a saturation. More precisely, the kinetic modeling indicates that only Pt is able to create the hydride species active in desorption of the isocarbenium. We think that the origin of this phenomenon is related to the distinction of the Y sites able to accept hydride ions. In the development of the kinetic equation, we assumed already the existence of YH^-_{Pt} and YH^-_{isom} sites. It is difficult to understand why on the same Lewis site Y, YH^-_{isom} is unreactive and only the YH^-_{Pt} is responsible for the isomerization activity. Therefore, we presume that it concerns two different sites. Maybe, the YH^-_{Pt} species can be associated directly with some specific Pt species. Taking into account these considerations, particularly substituting (YH^-) by (PtH^-) in the kinetic treatment, does not change the final rate expression. The identification of such a specific platinum species in sulfated zirconia, which limits the efficiency of the hydrogen activation, is presently under investigation and is the subject of a forthcoming publication.

CONCLUSION

The influence of hydrogen on the isomerization of *n*-hexane over Pt-enriched sulfated zirconia is modeled kinetically in a wide range of hydrogen and *n*-hexane partial pressures by a Lewis acid–base pair mechanism. Lewis sites are evidenced by IR characterization of the samples. Initiation occurs by hydride abstraction on a Lewis acid site and the isocarbenium is desorbed by a hydride originated from dissociation of hydrogen on platinum. The maximum in activity with respect to hydrogen pressure is well fitted by a very simple three-parameter rate equation. The three parameters of the rate equation reflect the number of sites, the acid strength, and the efficiency of platinum. In the series of catalysts examined, the acidity is constant while the platinum efficiency increases with Pt loading and reaches an upper limit at 0.15% platinum loading.

This simple kinetic model is a useful tool to guide the preparation of isomerization catalysts with respect to acidity and platinum efficiency and allows the effect of various poisons (H_2O, sulfur, NH_3) and coreactants (naphthenes) on the catalyst activity to be followed.

APPENDIX: KINETIC EQUATION

The reaction rate is given by the closed sequence (Scheme 2), in which the isomerization step is treated as a pseudo equilibrium.

$$r = r_i = k_i \cdot (X) \cdot (Y) \cdot (RH)$$

$$K = \frac{(XiR^+)}{(XR^+)}$$

$$r = r_t = k_t \cdot (XiR^+) \cdot (YH^-)$$

In the termination step, YH^- species are issued from both hydrocarbon and hydrogen. For sake of clarity, we separate the two terms, i.e.,

$$r_t = (XiR^+) \cdot (k_{t1} \cdot (YH^-)_{Pt} + k_{t2} \cdot (YH^-)_{isom}).$$

Then r_i is more convenient than r_t to express the reaction rate.

The total number of sites X and Y are assumed to be equal, because the active site is identified as an acid–base Lewis pair.

Then, $L_X = L_Y$, i.e.,

$$(X) + (XH^+) + (XR^+) + (XiR^+) = (Y) + (YH^-).$$

From electroneutrality,

$$(XH^+) + (XR^+) + (XiR^+) = (YH^-),$$

it becomes

$$(X) = (Y)$$

and the reaction rate becomes

$$r = k_i \cdot (X)^2 \cdot (RH).$$

In the site balance L_X, (XR^+) and (XiR^+) are linked by the equilibrium constant K, and (XiR^+) can be expressed

as a function of (X) from the equality $r_i = r_t$:

$$L_X = (X) + (XH^+) + \frac{k_i \cdot (1 + 1/K) \cdot (X)^2 \cdot (RH)}{k_{t1} \cdot (YH^-)_{Pt} + k_{t2} \cdot (YH^-)_{isom}}.$$

We need now to treat the platinum–hydrogen system to express (XH^+) and $(YH^-)_{Pt}$.

Activation of hydrogen on Pt and migration to the active sites is necessarily equilibrated because there is no hydrogen consumption in the isomerization reaction.

The appropriate rate equation is obtained by gathering in a single reaction the platinum–hydrogen system, owing to the fact that hydrogen migrates as a couple of atoms to reach the acid–base Lewis pair.

$$XY + H_2 \overset{Pt}{\leftrightarrow} XH^+YH^-$$

Since the only source of XH^+ is hydrogen involved in the couple XH^+YH^-, the concentration of XH^+ is necessarily equal to that of the couples XH^+YH^-. Similarly, the concentration of the free sites, X, should be equal to the concentration of the free couples, XY. Then

$$\alpha = \frac{(XH^+YH^-)}{(XY) \cdot (H)} = \frac{(XH^+)}{(X) \cdot (H)},$$

which allows us to express (XH^+) as a function of (X):

$$(XH^+) = \alpha \cdot (X) \cdot (H).$$

Consequently,

$$(YH^-)_{Pt} = \alpha \cdot (X) \cdot (H).$$

The total number of sites becomes

$$L_X = (X) + \alpha \cdot (X) \cdot (H) + \frac{k_i \cdot (1 + 1/K) \cdot (X)^2 \cdot (RH)}{k_{t1} \cdot \alpha \cdot (X) \cdot (H) + k_{t2} \cdot (YH^-)_{isom}}.$$

Recalling that $(YH^-)_{isom} = (XR^+) + (XiR^+)$, we can solve the second-order equation for $(YH^-)_{isom}$.

Introducing into L_X leads finally to

$$L_X = (X) \cdot \left\{ 1 + \alpha \cdot (H) + \frac{2 \cdot \beta \cdot (RH)}{\alpha \cdot (H) + \sqrt{\alpha^2 \cdot (H)^2 + 4 \cdot \beta \cdot \frac{k_{t2}}{k_{t1}} \cdot (RH)}} \right\},$$

in which

$$\beta = (1 + 1/K) \cdot \frac{k_i}{k_{t1}}.$$

Finally, the isomerization rate $r_i = k_i \cdot (X)^2 \cdot (RH)$ is expressed as

$$r = \frac{k_i \cdot L_X^2 \cdot (RH)}{\left\{ 1 + \alpha \cdot (H) + \frac{2 \cdot \beta \cdot (RH)}{\alpha \cdot (H) + \sqrt{\alpha^2 \cdot (H)^2 + 4 \cdot \beta \cdot \frac{k_{t2}}{k_{t1}} \cdot (RH)}} \right\}^2}.$$

Optimization of the kinetic parameters leads to a very low value of the ratio k_{t2}/k_{t1}. Then, the second term under the square root becomes negligible in front of $\alpha^2(H)^2$. This leads to the simplified rate equation with three parameters k, α and β,

$$r = \frac{k \cdot (RH)}{\left\{ 1 + \alpha \cdot (H) + \frac{\beta \cdot (RH)}{\alpha \cdot (H)} \right\}^2},$$

which fits all our data as shown in the figures.

REFERENCES

1. UOP web site: www.uop.com.
2. Arata, K., *Adv. Catal.* **37**, 165 (1990).
3. Tanabe, K., Hattori, H., and Yamaguchi, T., *Crit. Rev. Surf. Chem.* **1**, 1 (1990).
4. Yamaguchi, T., *Appl. Catal.* **61**, 1 (1990).
5. Corma, A., *Chem. Rev.* **95**, 559 (1995).
6. Davis, B. H., Keogh, R. A., and Srinivasan, R., *Catal. Today* **20**, 219 (1994).
7. Song, X., and Sayari, A., *Catal. Rev. Sci. Eng.* **38**, 329 (1996).
8. Wen, M. Y., Wender, I., and Tierney, J. W., *Energy Fuels* **4**, 372 (1990).
9. Ebitani, K., Hattori, H., and Tanabe, K., *Langmuir* **6**, 1743 (1990).
10. Ebitani, K., Konishi, J., and Hattori, H., *J. Catal.* **130**, 257 (1991).
11. Ebitani, K., Tsuji, J., Hattori, H., and Kita, H., *J. Catal.* **135**, 609 (1992).
12. Iglesia, E., Soled, S. L., and Kramer, G. M., *J. Catal.* **144**, 238 (1993), doi:10.1006/jcat.1993.1327.
13. Iglesia, E., Barton, D. G., Soled, S. L., Miseo, S., Baumgarter, J. E., Gates, W. E., Fuentes, G. A., and Meitzner, G. D., *Stud. Surf. Sci. Catal.* **101**, 533 (1996).
14. Comelli, R. A., Finelli, Z. R., Vaudagna, S. R., and Figoli, N. R., *Catal. Lett.* **45**, 227 (1997).
15. Duchet, J. C., Guillaume, D., Monnier, A., van Gestel, J., Szabo, G., Nascimento, P., and Decker, S., *Chem. Commun.* 1819 (1999).
16. Duchet, J. C., Guillaume, D., Monnier, A., van Gestel, J., Szabo, G., Nascimento, P., and Decker, S., *Div. Petr. Chem.* **44**, 425 (1999).
17. Olindo, R., Pinna, F., Strukul, G., Canton, P., Riello, P., Cerrato, G., Meligrana, G., and Morterra, C., *Stud. Surf. Sci. Catal.* **130**, 2375 (2000).
18. Duchet, J. C., Tilliette, M. J., and Cornet, D., *Catal. Today* **10**, 507 (1991), and Ref. 22 therein.
19. Zalewski, D. J., Alerasool, S., and Doolin, P. K., *Catal. Today* **53**, 419 (1999).
20. ASTM files 27-997, 17-923, and 37-1484.
21. Pinna, F., Signoretto, M., Strukul, G., Cerrato, G., and Morterra, C., *Catal. Lett.* **26**, 339 (1994).
22. Morterra, C., Cerrato, G., Pinna, F., Signoretto, M., and Strukul, G., *J. Catal.* **149**, 181 (1994), doi:10.1006/jcat.1994.1283.

23. Spielbauer, D., Mekhemer, G. A. H., Zaki, M. I., and Knözinger, H., *Catal. Lett.* **40**, 71 (1996).
24. Gates, B. C., Katzer, J. R., and Schuit, G. C. A., *in* "Chemistry of Catalytic Processes" (R. Ciofalo, D. J. Marshall, and B. Leap, Eds.), p. 280. McGraw–Hill, New York, 1979.
25. Guisnet, M., Fouché, V., Belloum, M., Bournonville, J. P., and Travers, C., *Appl. Catal.* **71**, 295 (1991).
26. Chu, H. Y., Rosynek, M. P., and Lunsford, J. H., *J. Catal.* **178**, 352 (1998), doi:10.1006/jcat.1998.2136.
27. Shishido, T., and Hattori, H., *Appl. Catal.* **146**, 157 (1996).
28. Yadav, G. D., and Nair, J. J., *Microporous Macroporous Mater.* **33**, 1 (1999).
29. Corma, A., *Chem. Rev.* **95**, 559 (1995), and references therein.
30. Anquetil, R., Ph.D. thesis, University of Caen (1998).
31. Nascimento, P., Akratopoulou, C., Oszagyan, M., Coudurier, G., Travers, C., Joly, J. F., and Védrine, J. C., *in* "New Frontiers in Catalysis" (L. Guczi, F. Solymosi, and P. Ttnyi, Eds.), p. 1185. Elsevier, Amsterdam, 1993.
32. Signoretto, M., Pinna, F., Strukul, F., Chies, P., Cerrato, G., Di Ciero, S., and Morterra, C., *J. Catal.* **167**, 522 (1997), doi:10.1006/jcat.1997.1575.
33. Liu, H., Adeeva, V., Lei, G. D., and Sachtler, W. M. H., *J. Mol. Catal.* **100**, 35 (1995).